Article

Cell Reports

Androgen Receptor Deregulation Drives Bromodomain-Mediated Chromatin Alterations in Prostate Cancer

Graphical Abstract

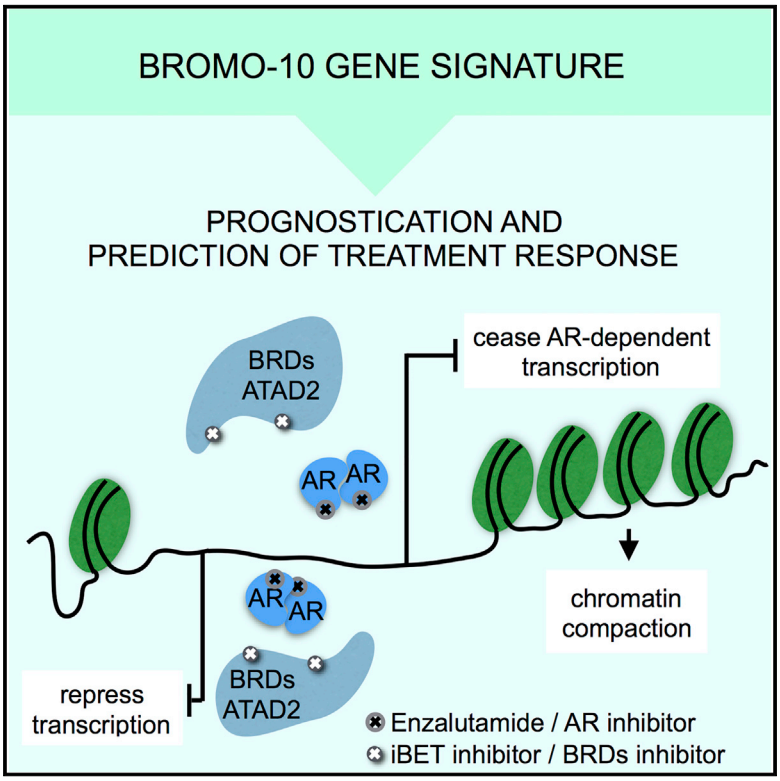

Highlights

- Androgen receptor (AR) overexpression drives genome-wide chromatin relaxation
- Bromodomain (BRD) inhibitors reduce local chromatin opening at AR target genes
- AR overexpression upregulates BRD proteins ATAD2, BRD2, and BRD4
- The BROMO-10 gene signature stratifies patients for therapy with BRD inhibitors

Authors

Alfonso Urbanucci, Stefan J. Barfeld, Ville Kytölä, ..., Matti Nykter, Tapio Visakorpi, Ian G. Mills

Correspondence

alfonsourbanucci@gmail.com (A.U.), i.g.mills@ncmm.uio.no (I.G.M.)

In Brief

Urbanucci et al. report how upregulated androgen receptor (AR) and AR-targeted bromodomain proteins contribute to genome-wide chromatin relaxation and increased gene transcription in advanced prostate cancer. They show that ATAD2 is a strong tissue biomarker and propose a BROMO-10 gene signature to stratify patients for combination therapies with bromodomain inhibitors.

Accession Numbers

GSE73989

Urbanucci et al., 2017, Cell Reports *19*, 2045–2059
June 6, 2017
http://dx.doi.org/10.1016/j.celrep.2017.05.049

Cell Reports
Article

Androgen Receptor Deregulation Drives Bromodomain-Mediated Chromatin Alterations in Prostate Cancer

Alfonso Urbanucci,[1,2,*] Stefan J. Barfeld,[1] Ville Kytölä,[3] Harri M. Itkonen,[1] Ilsa M. Coleman,[4] Daniel Vodák,[5] Liisa Sjöblom,[6] Xia Sheng,[7] Teemu Tolonen,[8] Sarah Minner,[9] Christoph Burdelski,[10] Kati K. Kivinummi,[3] Annika Kohvakka,[6] Steven Kregel,[11,12] Mandeep Takhar,[13] Mohammed Alshalalfa,[13] Elai Davicioni,[13] Nicholas Erho,[13] Paul Lloyd,[14,15] R. Jeffrey Karnes,[16] Ashley E. Ross,[17] Edward M. Schaeffer,[18] Donald J. Vander Griend,[11] Stefan Knapp,[19,20] Eva Corey,[21] Felix Y. Feng,[14,15,22] Peter S. Nelson,[4,21,23] Fahri Saatcioglu,[7,24] Karen E. Knudsen,[25] Teuvo L.J. Tammela,[26] Guido Sauter,[9] Thorsten Schlomm,[27] Matti Nykter,[3] Tapio Visakorpi,[6] and Ian G. Mills[1,2,28,29,*]

[1]Centre for Molecular Medicine Norway, Nordic European Molecular Biology Laboratory Partnership, Forskningsparken, University of Oslo, 21 0349 Oslo, Norway
[2]Department of Molecular Oncology, Institute for Cancer Research, Oslo University Hospital, 0424 Oslo, Norway
[3]Prostate Cancer Research Center, Institute of Biosciences and Medical Technology (BioMediTech), University of Tampere and Tampere University of Technology, 33520 Tampere, Finland
[4]Division of Human Biology, Fred Hutchinson Cancer Research Center, Seattle, WA 98109, USA
[5]Department of Tumor Biology, Institute for Cancer Research, The Norwegian Radium Hospital, Oslo University Hospital, 0424 Oslo, Norway
[6]Prostate Cancer Research Center, Institute of Biosciences and Medical Technology (BioMediTech), University of Tampere and Fimlab Laboratories, Tampere University Hospital, 33520 Tampere, Finland
[7]Department of Biosciences, University of Oslo, 0316 Oslo, Norway
[8]Department of Pathology, Fimlab Laboratories, Tampere University Hospital, 33520 Tampere, Finland
[9]University Medical Center Hamburg-Eppendorf, 20251 Hamburg, Germany
[10]General, Visceral and Thoracic Surgery Department and Clinic, University Medical Center Hamburg-Eppendorf, 20246 Hamburg, Germany
[11]Department of Surgery - Section of Urology, University of Chicago, Chicago, IL 60637, USA
[12]Michigan Center for Translational Pathology, University of Michigan, Ann Arbor, MI 48109-0940, USA
[13]Research and Development, GenomeDx Biosciences, Vancouver, BC V6B 1B8, Canada
[14]Department of Medicine, University of California at San Francisco, San Francisco, CA 94143-0410, USA
[15]Helen Diller Comprehensive Cancer Center, University of California, San Francisco, CA 94143-0981, USA
[16]Department of Urology, Mayo Clinic, Rochester, MN 55902, USA
[17]Brady Urological Institute, Johns Hopkins Medical Institute, Baltimore, MD 21287, USA
[18]Department of Urology, Northwestern University, Feinberg School of Medicine, 303 East Chicago Avenue, Tarry 16-703, Chicago, IL 60611-3008, USA
[19]Nuffield Department of Clinical Medicine, University of Oxford, Old Road Campus, Roosevelt Drive, Oxford OX3 7DQ, UK
[20]Institute for Pharmaceutical Chemistry, Goethe-University Frankfurt, Campus Riedberg, Max-von Laue Strasse 9, 60438 Frankfurt am Main, Germany
[21]Department of Urology, University of Washington, Seattle, WA 98195, USA
[22]Department of Radiation Oncology, University of California, San Francisco, San Francisco, CA 94115, USA
[23]Department of Pathology, University of Washington, Seattle, WA 98195, USA
[24]Institute for Cancer Genetics and Informatics, Oslo University Hospital, 0424 Oslo, Norway
[25]Sidney Kimmel Cancer Center, Thomas Jefferson University, Philadelphia, PA 19107, USA
[26]Prostate Cancer Research Center and Department of Urology, University of Tampere and Tampere University Hospital, 33014 Tampere, Finland
[27]Martini-Clinic, Prostate Cancer Center, University Medical Center Hamburg-Eppendorf, Hamburg 20095, Germany
[28]PCUK Movember Centre of Excellence, CCRCB, Queen's University, Belfast BT7 1NN, Northern Ireland, UK
[29]Lead Contact
*Correspondence: alfonsourbanucci@gmail.com (A.U.), i.g.mills@ncmm.uio.no (I.G.M.)
http://dx.doi.org/10.1016/j.celrep.2017.05.049

SUMMARY

Global changes in chromatin accessibility may drive cancer progression by reprogramming transcription factor (TF) binding. In addition, histone acetylation readers such as bromodomain-containing protein 4 (BRD4) have been shown to associate with these TFs and contribute to aggressive cancers including prostate cancer (PC). Here, we show that chromatin accessibility defines castration-resistant prostate cancer (CRPC). We show that the deregulation of androgen receptor (AR) expression is a driver of chromatin relaxation and that AR/androgen-regulated bromodomain-containing proteins (BRDs) mediate this effect. We also report that BRDs are overexpressed in CRPCs and that ATAD2 and BRD2 have prognostic value. Finally, we developed gene stratification

signature (BROMO-10) for bromodomain response and PC prognostication, to inform current and future trials with drugs targeting these processes. Our findings provide a compelling rational for combination therapy targeting bromodomains in selected patients in which BRD-mediated TF binding is enhanced or modified as cancer progresses.

INTRODUCTION

Prostate cancer (PC) is the most common male cancer in the United States and Europe (Center et al., 2012). Androgen receptor (AR) signaling is required for the development of the prostate gland and is maintained in PC including at the stage of progression to castration-resistant prostate cancer (CRPC) (Zhang et al., 2013).

CRPC is characterized by copy number gain at the AR locus occurring in around 30% of advanced cases. Consequently AR is overexpressed in these tumors. However, AR deregulation is also a frequent feature (>90%) of advanced castrate-resistant cases (Waltering et al., 2012), which persist after resistance to antiandrogens such as enzalutamide and abiraterone (Buttigliero et al., 2015). We have previously shown that AR deregulation is associated with local chromatin landscape changes, which are able to reinforce the binding of AR to chromatin even in low androgen environments (Urbanucci et al., 2012a, 2012b). This mimics the conditions occurring in CRPC (Xu et al., 2006). Phenotypically, AR deregulation results in increased growth rates even under conditions of androgen deprivation (Waltering et al., 2009). Moreover, genome-wide AR recruitment to chromatin is detectable in such conditions (Andreu-Vieyra et al., 2011), suggesting that the chromatin is open and in some way primed by pre-docked AR even before the cells are treated with hormones. Androgen treatment then enhances AR recruitment (Urbanucci et al., 2012a). This suggests that nucleosome positioning is predetermined in PC cells, a hypothesis that has been confirmed by a recent study (Chen et al., 2015).

Clinical epigenetics, defined as functionally relevant changes to the genome that do not involve a change in the nucleotide sequence and impact on disease phenotypes, is becoming extremely important for cancer detection and treatment. One indirect assessment of epigenetic alteration is the accessibility of DNA, determined by DNase hypersensitivity analysis or by formaldehyde-assisted isolation of regulatory elements (FAIREs) (Song et al., 2011).

Proof of a de-regulated epigenome in CRPC includes altered patterns of DNA methylation, histone modifications (Perry et al., 2010), and increased and altered AR binding to chromatin (Pomerantz et al., 2015; Sharma et al., 2013).

In addition, epigenetic readers such as bromodomain-containing protein 4 (BRD4) have been shown to associate with transcription factors (TFs) such as AR (Asangani et al., 2014; Nagarajan et al., 2014; Shi and Vakoc, 2014) and contribute to aggressive cancers of many types (Delmore et al., 2011; Shi and Vakoc, 2014) including PC (Asangani et al., 2014; Wyce et al., 2013). Nevertheless, the underlying mechanisms of action of bromodomain inhibitors have not yet been completely elucidated (Shi and Vakoc, 2014). Therefore, we set out to investigate the underlying global changes in chromatin accessibility as a driver of cancer progression (Lever and Sheer, 2010; Timp and Feinberg, 2013).

Here, we report that DNA accessibility alone is able to discriminate advanced prostate tumors from earlier disease states and benign tissue. The chromatin of these tumors is more accessible due to indirect mechanisms in which the AR plays a role. We show that BRDs, such as BRD4 and androgen-regulated BRD2 and ATAD2, are the mediators of such increased accessibility and are prognostic tissue markers overexpressed in CRPC. Finally we provide a ten-gene signature, BROMO-10, that can be used to stratify patients with poorer outcome and guide PC patient selection for combinatorial trials of bromodomain and extra-terminal (BET)-targeted therapies with other agents.

RESULTS

Deregulation of the AR Enhances Bromodomain-Mediated Chromatin Opening in Advanced Tumors

To understand whether progression to CRPC is associated with global changes in chromatin accessibility, we assessed chromatin opening and DNA regions with regulatory activity in three benign prostate hyperplasia (BPH), three primary untreated PC, and three locally recurrent CRPC samples using FAIRE sequencing (FAIRE-seq) (Giresi and Lieb, 2009).

One-third of the genome consisted of open regions of chromatin in two CRPC samples, whereas only about one-sixth of the genome comprised open chromatin in the other samples (Figure 1A and Table S1A). We validated open chromatin regions via FAIRE-qPCR at prostate specific antigen (PSA) and TMPRSS2 gene loci, showing enhanced chromatin opening in CRPC (Figure 1B).

We built disease-stage-specific high-confidence consensus open chromatin maps. On average, only 15% of the FAIRE-seq sites overlapped between the samples (Table S1A) highlighting epigenetic heterogeneity. We found that the majority of open sites were unique to CRPC samples (Figure 1C) and were larger than in PC or BPH (Figure S1A). To classify disease stage, we used principal component analysis of the FAIRE-seq data and found that in terms of chromatin state, CRPC chromatin appeared more diverse when compared with BPH or PC (Figure 1D), indicating that extensive chromatin remodeling is a late event in PC progression.

RNA sequencing (RNA-seq) of the same clinical samples showed a positive correlation between upregulated genes and an open chromatin state (Figure 1E) up to 250 kb upstream the transcriptional start sites (TSSs) (Figure 1F). In agreement with published studies (Cedar and Bergman, 2012), DNA methylation profiles obtained for the same clinical samples showed a negative correlation with gene expression within 1 and 5 kb around the genes' TSS (Figure 1G). Importantly, such correlations were independent of sample type, indicating conserved mechanisms across all disease stages.

Next, to investigate the effect of the AR deregulation on chromatin opening, we performed FAIRE-seq in CRPC cells such as lymph node carcinoma of the prostrate (LNCaP) and

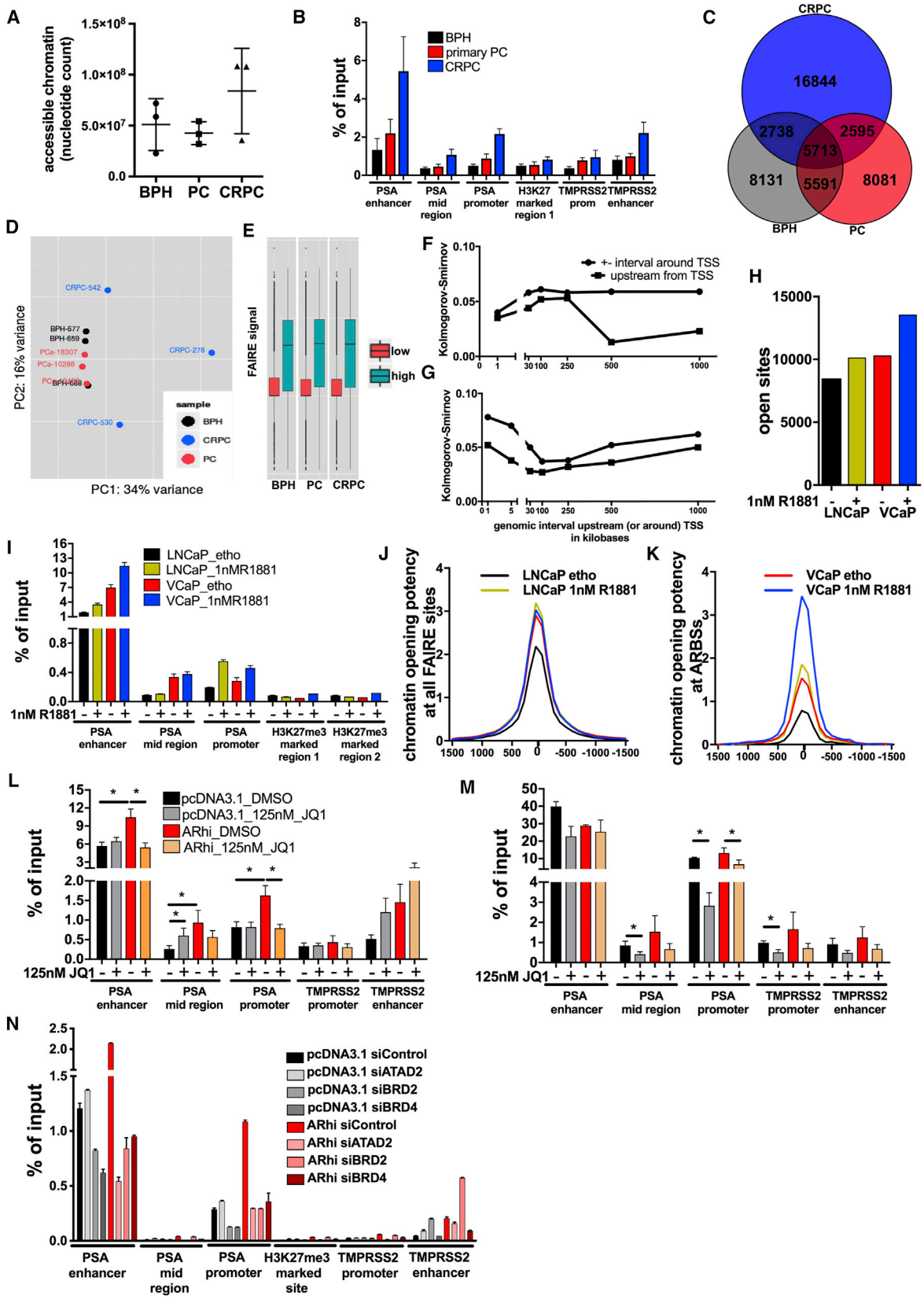

(legend on next page)

vertebral-cancer of the prostate (VCaP) cultured in the presence and absence of androgens. VCaP cells overexpress the AR compared to LNCaP due to AR gene locus amplification (Urbanucci et al., 2013). More FAIRE-seq sites were found in VCaP than in LNCaP cells (Figure 1H and Table S1A), and VCaP cells also showed a greater increase in the number of FAIRE-seq sites in the presence of androgens (Figure 1H).

One-third of the FAIRE-seq sites were present in both cell lines (Figure 2A). Androgen treatment reprogrammed chromatin accessibility affecting 20%–50% of sites (Figure 2B).

80% of common FAIRE-seq sites were conserved between cell lines and tissue samples (Table S1B). Chromatin opening measured via FAIRE-qPCR at PSA (Figure 1I) and TMPRSS2 (Figure 2C) loci or measured in silico genome-wide (Figures 1J and 2D–2F) was greater in VCaP cells than in LNCaP cells. An average of 21% of clinically relevant AR binding sites (ARBSs) in CRPC tissue (Sharma et al., 2013) and 45% E26 transformation-specific or E-twenty-six family (ETS)-related gene (ERG) binding sites (ERGBSs) in VCaP cells (from Yu et al., 2010) overlapped with FAIRE sites (Table S1B).

Androgens enhanced chromatin opening at FAIRE sites overlapping with CRPCs' ARBSs and ERGBSs only in LNCaP cells (Figures 2D and 2E), while they had no effect in VCaP cells. In VCaP cells, androgens enhanced chromatin opening at matched cell lines ARBSs (Figure 1K) and at ARBSs present in cell lines and tumors (Figure 2F) but not at ERGBSs (Figure 2E).

To validate the role of AR in chromatin opening, we used an LNCaP-based model expressing endogenous and increased AR levels (Waltering et al., 2009) (Figure 2G) and confirmed enhanced chromatin opening in AR-overexpressing cells at the PSA and TMPRSS2 loci. These data suggest that both AR deregulation and androgens affect chromatin opening in CRPC cells at ARBSs, but not at ERGBSs.

Distribution of FAIRE-seq sites in clinical samples and cell lines showed increased opening at intronic/intergenic regions (Figures S1B–S1I), which is in agreement with previous findings showing increased AR chromatin binding at these regions (Sharma et al., 2013; Urbanucci et al., 2012b).

Given that chromatin remodeling is not exclusively associated with ARBSs, we tested whether enhanced chromatin opening was associated with the presence of different motifs in CRPC by performing motif analysis on FAIRE site maps of tissue samples and cell lines (Table S1C). Consistent with its role in maintaining chromatin compaction (Tark-Dame et al., 2014), CCCTC-binding factor (CTCF)-like motifs were among the top enriched motifs in both clinical specimens and cell lines, followed by ETS-like motifs. CTCF and ETS motifs were enriched in all clinical specimens, including common sites, while c-MYC motifs were exclusively present in open regions found in CRPC samples. Nuclear transcription factor Y subunit (NFY) and SP1 motifs were highly enriched in both treatment conditions in both cell lines. Although they were not enriched at FAIRE sites in tumors, NFY and SP1 have been shown to be involved in chromatin regulation and to have a potential role in cancer progression (Dolfini and Mantovani, 2013; Tewari et al., 2012). Interestingly, forkhead box (FOX)-like motifs were significantly enriched only in the LNCaP FAIRE sites (Table S1C). This suggests that only a subset of FAIRE sites, those that may overlap with ARBSs, are regulated by FOXA1, and other chromatin remodelers may play a role.

Therefore, we sought to understand whether enhanced chromatin opening in the context of AR deregulation favors chromatin binding of different proteins such as nuclear transcription factor Y subunit alpha (NFYA), the regulatory subunit of the NFY complex (Dolfini and Mantovani, 2013), and c-Myc.

We retrieved publicly available consensus binding data from ENCODE. Overlap of FAIRE-seq data with ENCODE data on chromatin binding of CTCF, MYC, and NFYA showed that, on average, 44% of the ENCODE NFYA sites, 18% of MYC sites, and only 12% of CTCF sites lay within the open chromatin sites (Table S1D). However, no significant increase or decrease of overlapping sites was observed in CRPCs, which may be due

Figure 1. Deregulation of AR Favors Bromodomain-Mediated Chromatin Opening in Castration-Resistant Prostate Cancer

(A) Number of nucleotides located within open chromatin peaks identified via formaldehyde-assisted isolation of regulatory elements followed by sequencing (FAIRE-seq) in three benign prostate hyperplasia (BPH), three primary prostate cancer (PC), and three locally recurrent castration-resistant prostate cancer (CRPC) tissue specimens.

(B) FAIRE-qPCR validation of local chromatin opening at the PSA and TMPRSS2 loci in the clinical samples. An H3K27me3 marked region was used as negative control (closed region).

(C) Overlap of open chromatin regions commonly found in BPH, PC, or CRPC samples according to the FAIRE-seq analysis.

(D) Principal component analysis of three benign and six cancer (three primary and three CRPC) prostate tissue samples according to chromatin shape.

(E) Association between local chromatin opening, up to 1 kb upstream the genes transcription start site, and gene expression in matched tissue samples, according to RNA-seq.

(F and G) Analysis of Kolmogorov-Smirnov statistical test values describing the deviation of correlative events between matched gene expression and local chromatin accessibility (F) or local DNA methylation (G) from a random set of associative events of the same type, in all nine clinical samples. Local chromatin accessibility and DNA methylation were measured at the indicated intervals and correlated in a gene-wise manner to respective gene expression in the same tissue (see Figure S4 for details).

(H) Number of open chromatin regions found by FAIRE-seq analysis of LNCaP and VCaP cells treated with 1 nM R1881 or vehicle.

(I) FAIRE-qPCR validation of local chromatin opening at the PSA locus in LNCaP and VCaP cells treated with 1 nM R1881 or vehicle.

(J and K) Chromatin opening potency assessed by FAIRE-seq reads distribution around all FAIRE-seq sites (J) or around matched androgen receptor binding sites (ARBSs) (K) in LNCaP and VCaP cells treated as above.

(L–N) FAIRE-qPCR analysis of local chromatin opening at the PSA and TMPRSS2 loci in a LNCaP-based AR overexpression model (*$p < 0.05$ according to t test). FAIRE-qPCR in LNCaP-pcDNA3.1 and -ARhi cells following 4 days of hormone starvation (L) or without starvation (full serum) (M), treated with 125 nM JQ1 (+) or vehicle (DMSO) (–) (*$p < 0.05$ according to t test). (N) FAIRE-qPCR upon transfection with siRNA control or siRNA against ATAD2 (siATAD2), BRD2 (siBRD2), or BRD4 (siBRD4) (two biological repeats with three technical replicates each).

Error bars represent SEM. See also Figure S1 and Tables S1A–S1D.

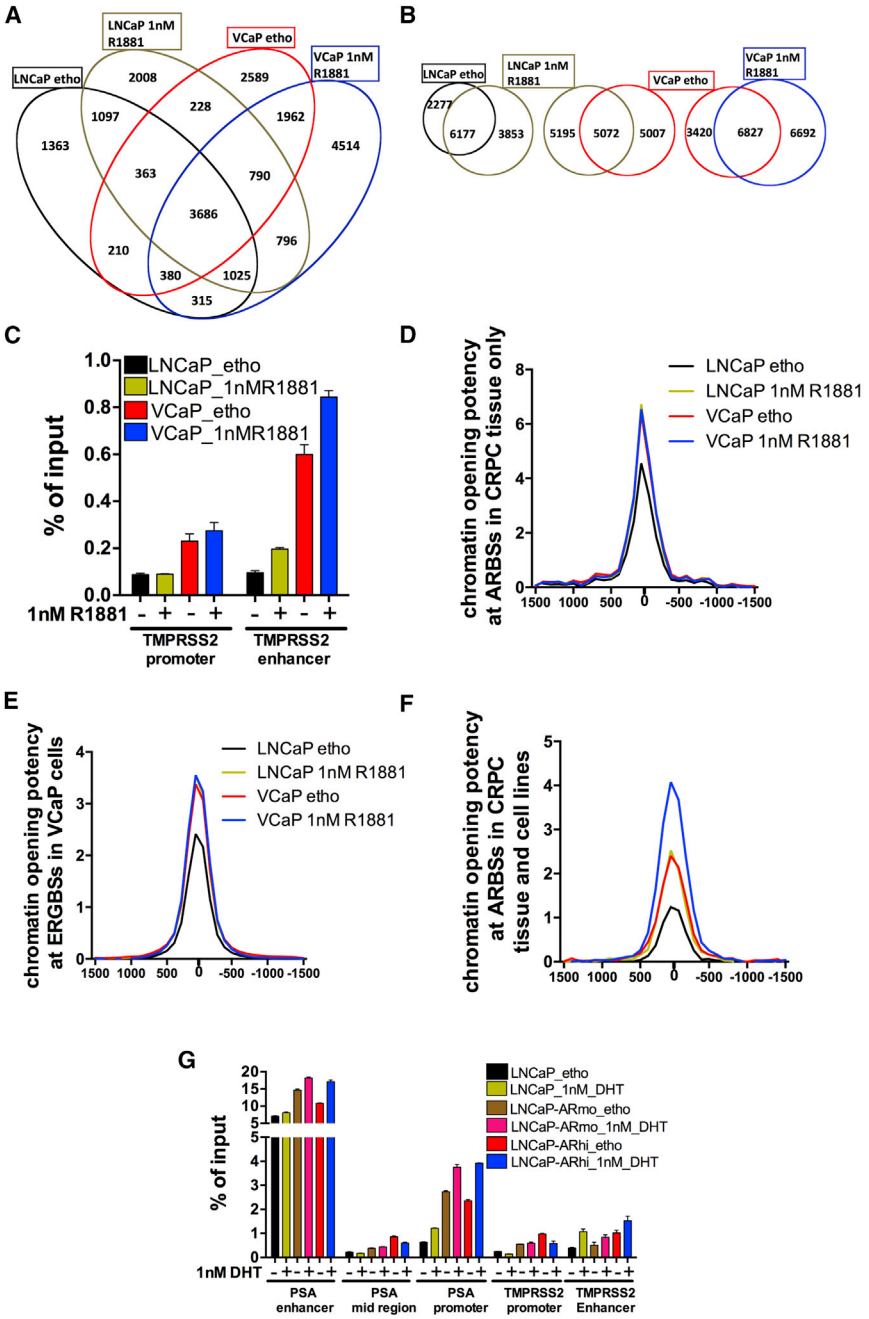

Figure 2. AR Overexpression in Castration-Resistant PC Cell Models Is Associated with Increased Open Chromatin

(A and B) Multi-parametric comparison showing open chromatin regions found by FAIRE-seq analysis in LNCaP and VCaP cells treated with 1 nM R1881 or vehicle (etho, ethanol) (A). Three pairwise comparisons of open chromatin regions—LNCaP treated with R1881 or ethanol; LNCaP treated with R1881 versus VCaP treated with ethanol and VCaP treated with R1881 or ethanol (B).

(C) FAIRE-qPCR validation of local chromatin opening at the TMPRSS2 locus (Urbanucci et al., 2012a) in two cell lines with and without hormone or vehicle.

(D–F) Chromatin opening around (D) androgen receptor binding sites (ARBS) in CRPC (Sharma et al., 2013), (E) ERG binding sites (ERGBS) (Yu et al., 2010), and (F) ARBS conserved between CRPC tissue and cell lines (Sharma et al., 2013).

(G) FAIRE-qPCR validation of chromatin opening at PSA and TMPRSS2 loci (Urbanucci et al., 2012a) in a LNCaP-based AR overexpression model (Waltering et al., 2009) treated with hormone or vehicle.

Error bars represent SEM.

to cell specificity of the TF binding or due to tissue heterogeneity (data not shown).

BRDs are druggable chromatin readers that recognize acetylated histones (Filippakopoulos et al., 2012) and modulate transcription in cancer-associated genes (Filippakopoulos and Knapp, 2014; Lovén et al., 2013). Since we showed that histone acetylation is increased in AR-overexpressing cells (Urbanucci et al., 2012a), we hypothesized that BRDs would mediate chromatin opening. To test our hypothesis, we used the pan-BET bromodomain inhibitor JQ1 to assess the impact on chromatin opening potency at selected loci.

In hormone-starved cells, JQ1 treatment induced chromatin closure in AR-overexpressing cells, but had little or no effect in parental cells (Figure 1L). In the presence of androgens, JQ1 had a stronger effect on parental than on AR-overexpressing cells (Figure 1M), highlighting the role of androgens in chromatin opening. In addition to BRD2/4 as the main targets of JQ1, we also evaluated ATAD2, since it has been reported that this BRD is a common coactivator of AR and MYC.

RNAi knockdown of the BET proteins BRD2 and BRD4 reduced PSA enhancer and promoter opening in AR-overexpressing cells, but in parental cells ATAD2 knockdown did not (Figure 1N). Interestingly, at the TMPRSS2 enhancer only BRD4 knockdown was effective in reducing chromatin opening, suggesting that compensatory events occur if a specific BRD is targeted.

Based on these data, we hypothesized that the expression of some BRDs might be AR dependent. To test androgen regulation of BRDs genes we validated proximal ARBSs (Data S1) identified in publicly available datasets. Chromatin immunoprecipitation at ATAD2 and BRD2 proximal ARBSs showed stronger AR binding than BRD4 proximal ARBS. The strongest ARBS to BRD4 was located 200 kb from the TSS (Figure 3A). ATAD2 and BRD2 transcripts were induced by androgen (the latter only modestly), while BRD4 transcript was not (Figure 3B). AR

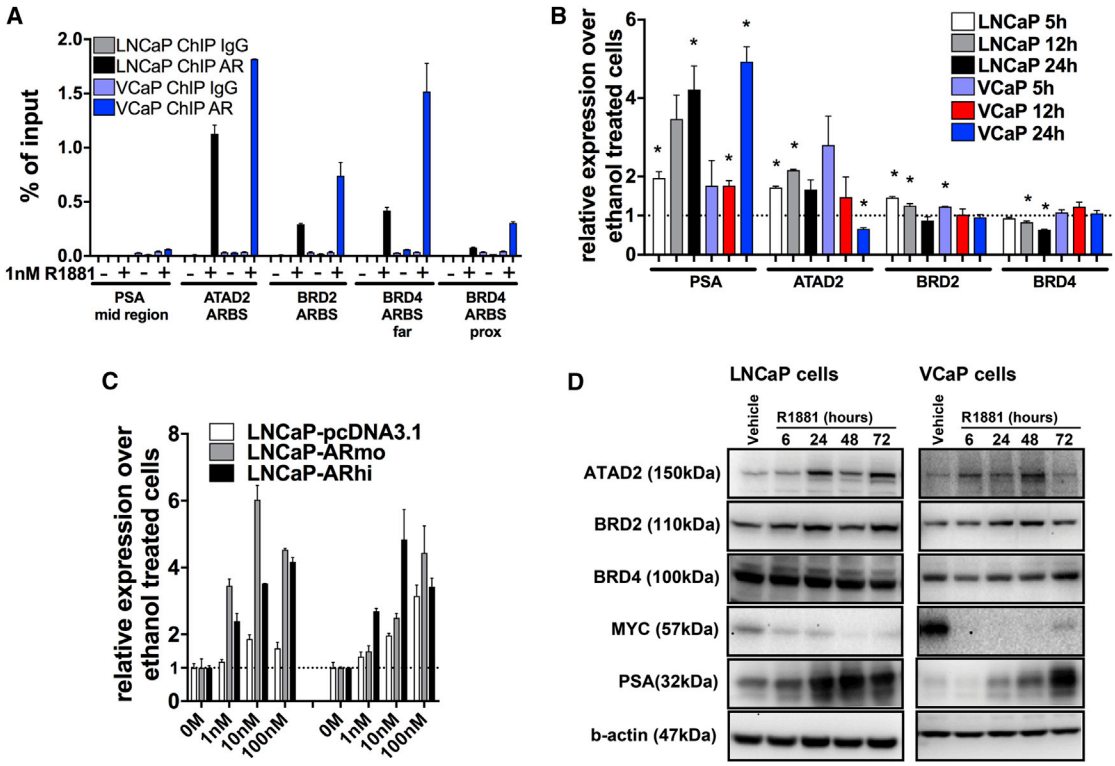

Figure 3. Androgens and AR Regulate BRDs Expression

(A) Androgen receptor binding sites (ARBSs) close to BRD4, BRD2, and ATAD2 genes according to publicly available datasets (see Data S1) were validated by chromatin immunoprecipitation (ChIP)-qPCR analysis. PSA mid-region served as ARBS negative control.

(B) Indicated transcript levels measured by qRT-PCR after hormone treatment.

(C) ATAD2 gene expression measured by qRT-PCR in LNCaP-pcDNA3.1, -ARmo, and -ARhi treated with hormone. The mean and SEM of ATAD2 against TATA-binding protein (TBP) values normalized measure with no treatment (0M).

(D) Western blot analysis of indicated proteins levels in cells treated with hormone.

See Figure S2.

overexpression sensitized ATAD2 transcription to lower concentrations of androgens (Figure 3C). In contrast to BRD4, ATAD2 and BRD2 protein levels were increased in AR-overexpressing cells and further increased by androgen stimulation (Figures 3D and S2A). AR knockdown in LNCaP cells during a time course of androgen treatment reduced ATAD2 transcript and protein levels within 24 hr (Figures S2B and S2C). In contrast, BRD2 protein levels were downregulated only after 48 hr treatment with AR-targeted small interfering RNA (siRNA) (Figure S2C).

BRDs Are Tissue Biomarkers Overexpressed in Castration-Resistant PCs

To establish the predictive clinical value of BRD2/4 and ATAD2, we performed qRT-PCR (Figures 4A–4D) and immunohistochemical (IHC) analyses (Figures 4E–4H) using benign prostate tissue and PC specimens and found that all transcripts were overexpressed in cancer compared to BPH. The long form of BRD4 (BRD4-L) ($p > 0.05$) and BRD2 ($p < 0.0001$) nuclear staining was increased in CRPC (Figures 4I and 4J). BRD4 (Figure S3A) and BRD2 (Figure 4K) protein levels determined by IHC were not prognostic for biochemical recurrence, although BRD2 staining separated patients with poor prognosis and was significantly ($p = 0.0154$) associated with mortality (Figure 4L). Strong nuclear (Figure 4M) and cytoplasmic (Figure S3B) staining for ATAD2 was significantly increased in CRPC cases ($p < 0.0001$). Moreover, strong nuclear (Figure 4N) but not cytoplasmic (Figure S3C) staining was associated with poor outcome (Figure S3D). We confirmed the significant ($p < 0.001$) prognostic relevance of ATAD2 as a tissue biomarker for biochemical recurrence in an independent cohort of 12,427 patients' samples (Figures 4O and S3). Positive staining for ATAD2 was associated with Ki67 staining, tumor stage, and AR protein expression (Figure S3).

Androgen-Receptor-Overexpressing Cells Are More Sensitive to Bromodomain Inhibitors

BRD inhibitors have been reported to reduce the viability of PC cells (Asangani et al., 2014). To determine whether these effects are dependent on AR expression levels, we performed knockdowns of BRDs in AR-overexpression cell models in the presence of androgens (Figures S4A and S4B). Silencing BRD4 decreased MYC levels in both LNCaP and VCaP cells, while upregulating slightly AR, and PSA only in VCaP cells (Figure S4B). Knockdown of BRD4 decreased viability in all the AR-positive cell lines tested (LNCaP-pcDNA3.1, LNCaP-ARhi, and VCaP),

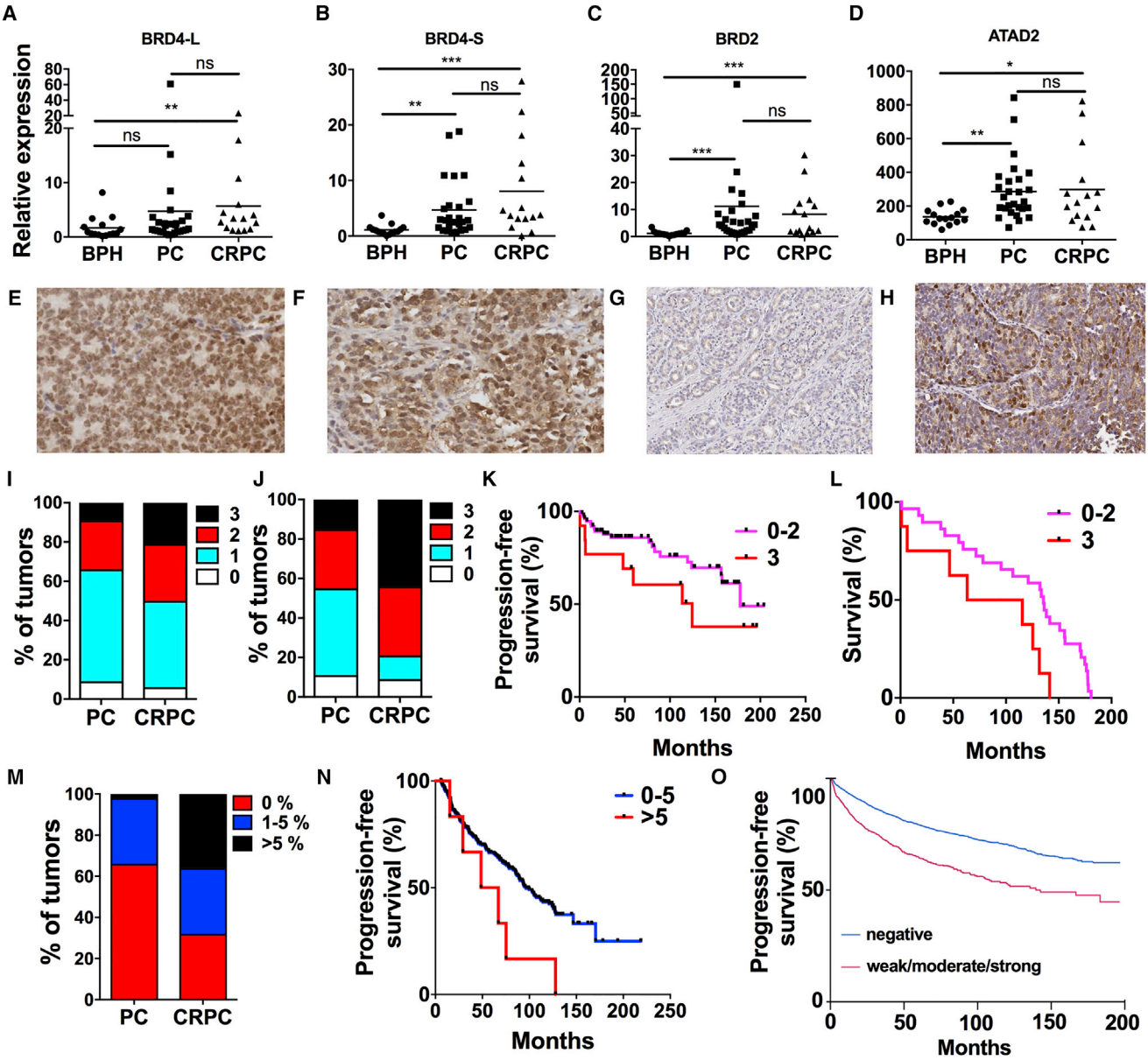

Figure 4. BRDs Are Tissue Biomarkers Overexpressed in Castration-Resistant PC

(A–D) Expression of BRD4-long (BRD4-L) (A), BRD4-short (BRD4-S) transcript form (B), BRD2 (C), and ATAD2 (D) gene transcripts relative to TBP levels in BPH (n = 15), primary untreated PC (n = 27), and CRPC (n = 15) specimens according to qRT-PCR. Kruskal-Wallis with Dunn post-test results are shown (***p < 0.0001; **p < 0.001; *p = 0.01–0.05; ns, not significant).

(E and F) CRPC immunohistochemical (IHC) strong stainings (score = 3) for BRD4 long isoform (E) and BRD2 (F).

(G and H) CRPC IHC stainings showing examples of low (0%) (G) and high (<5%) (H) staining of nuclear ATAD2. Images are 8× magnification.

(I and J) Proportions of tumors according to BRD4 long isoform (I) and BRD2 (J) staining intensity in PC (n = 159 for BRD4 and n = 90 for BRD2) and CRPC (n = 128 for BRD4 long isoform and n = 34 for BRD2).

(K) Kaplan-Meier analysis of biochemical progression-free survival in 90 prostatectomy-treated patients according to BRD2 stainings (p = ns calculated with Mantel-Cox test).

(L) Kaplan-Meier analysis showing shorter time to death in 37 men that died of PC out of the 90 patients for which material was stained for BRD2 (p = 0.015 calculated with Mantel-Cox test).

(M) Proportions of tumors according to percentage of ATAD2 positive nuclei in PC (n = 258) and CRPC (n = 121) specimens (p < 0.0001 according to X^2 test).

(N) Kaplan-Meier analysis of biochemical progression-free survival in prostatectomy-treated patients according to the percentage of ATAD2 positive nuclei. Six patients with high frequency of ATAD2-positive nuclei had very short progression-free time (p = 0.0354 calculated with Mantel-Cox test).

(O) Kaplan-Meier analysis of biochemical progression-free survival in a validation cohort of 8,541 prostatectomy-treated patients according to ATAD2 staining (p < 0.001). 26% (n = 2,216) of the stainings were positive for ATAD2, of which strong ATAD2 staining accounted for 81% (n = 1,789).

Error bars represent SEM. See Figure S3.

but knockdown of BRD2 or ATAD2 alone had no effect on viability (Figure 5A). ATAD2 inhibition via a small molecular probe was shown to have limited effect on viability of LNCaP cells (Bamborough et al., 2016). Silencing ATAD2 upregulated AR specifically in LNCaP and MYC in VCaP cells, while silencing BRD2 slightly upregulated MYC in both LNCaP and VCaP cells (Figure S4B). Therefore, our data suggest that compensatory mechanisms such as enhanced AR/MYC signaling may take place and promote cell survival when single BRDs are targeted. In fact, co-targeting both ATAD2 and BRD2 in LNCaP cells via a combinatorial knockdown had no additive effect on decreasing cell viability compared to targeting BRD2 alone (Figure 5B) and highlighted that BRD4 is important but not the only contributor to cell viability.

To test whether AR deregulation enhances sensitivity to bromodomain inhibitors, we treated a panel of AR-positive PC cell lines with JQ1 in the presence of androgens (Figures 5C, S4C, and S4D). AR levels in 22RV1 and LNCaP cells are similar (Erzurumlu and Ballar, 2017), while LNCaP-ARhi and VCaP cells overexpress AR compared to LNCaP (or LNCaP-pcDNA3.1) with VCaP showing the highest levels of AR (Urbanucci et al., 2012b; Waltering et al., 2009). VCaP cells were indeed the most sensitive cells to JQ1 treatment. LNCaP-ARhi and parental LNCaP cells were equally responsive to JQ1 treatment (Figure S4D). However, when such cells were grown in androgen deprivation conditions (castrate conditions), AR-overexpressing cells were more sensitive to JQ1 (Figure 5D). Also, combined treatment with enzalutamide and JQ1 was more effective in AR-overexpressing cells (Figures 5E and 5F), suggesting that AR deregulation is implicated in response to BET inhibition.

Combined treatment with JQ1 and enzalutamide triggered apoptosis in VCaP cells in full media (Figure 5G), but not in LNCaP cells, even when deprived of androgens (Figures S4E and S4F). This indicates that AR activity/level defines whether this drug combination has a cytostatic (low-level AR activation) or cytotoxic (high-level AR activation) effect.

When cells are treated with anti-androgens, resistance can emerge in which AR activity is maintained (Buttigliero et al., 2015). Using an enzalutamide-resistant LNCaP model (Kregel et al., 2013), we found that the inhibitory effect of JQ1 was retained (Figure 5H).

Gene Expression Analysis of Bromodomain Inhibitor-Treated Cells and Six Independent PC Cohorts Reveal a Ten-Gene Signature for Patient Stratification

To identify patients that could potentially benefit from BET-targeted therapies, we sought to identify a gene signature able to stratify CRPC responders. We performed a time-course treatment with JQ1 in LNCaP (Figure S5A) and VCaP (Figure S5B) cells to identify affected genes. Upregulated genes (Table S2A) showed significant overrepresentation of histone genes (Figures S5C and S5D) and overrepresentation of GO terms for chromatin compaction ($p < 10^{-6}$) (Table S3), corroborating the tendency for chromatin closure upon JQ1 treatment, while downregulated transcripts (Table S2B) included AR targets found in tissues of CRPC patients (Sharma et al., 2013) (Figure 6A). We validated decreased protein levels of the AR targets PSA and CAMKK2 upon JQ1 treatment (Figure S2A). CRPC-associated genes such as UBE2C, HOXB13, AURKA, and CAMKK2 (Data S1) that were downregulated by JQ1 treatment (Figures S5E and S5F) and affected by BRD4 knockdown (Figure S5G) also showed bromodomain-dependent local chromatin opening (Figure S5H). AR deregulation affected chromatin opening especially at ARBSs, when present (Figures S5I and S5J).

Finally, we used published clinical expression array data (Taylor et al., 2010) and RNA-seq of clinical specimens (Ylipää et al., 2015) to identify a clinical gene signature of overexpressed genes in CRPC (Tables S4A and S4B). We compared lists of CRPC-overexpressed genes with those that displayed increased proximal chromatin opening in CRPC (Figure 6B and Table S5) and genes downregulated by JQ1 treatment in cell lines and obtained a set of 15 genes (Figures 6C and 6D).

A generalized linear model with elastic net regularization (Erho et al., 2013) was used on the Mayo Clinic I (MCI) PC cohort (Erho et al., 2013) as the discovery dataset to assess the association of the 15 genes to biochemical recurrence, PC specific mortality, and metastatic recurrence. Ten of the 15 genes contributed significantly to the model.

We called the resulting ten-gene signature "BROMO-10." To evaluate the prognostic significance of BROMO-10, first we used RNA-seq data from an independent cohort of PC from the Fred Hutchinson Cancer Research Center (Kumar et al., 2016; Roudier et al., 2016) (Figures 6E and 6F). Genes comprising the signature were deregulated in this cohort with seven out of ten genes being differentially expressed when comparing CRPCs to primary PCs.

Next, we assessed the independent prognostic value of each gene according to various endpoints in two additional validation cohorts (Karnes et al., 2013; Ross et al., 2016) (Table S6).

According to univariable and multivariable analysis, BROMO-10 contributed independent prognostic information over the clinicopathological variables. In the Johns Hopkins Medical Institutions-Radical Prostatectomy (JHMI-RP) cohort of high-risk men treated with radical prostatectomy without adjuvant or salvage therapy prior to metastatic onset, BROMO-10 discriminated for the biochemical recurrence endpoint (Figures 7A, S6A, and S6B) and the PC-specific mortality endpoint in the MCII cohort of high-risk men (Figures 7B, S6C, and S6D).

We further assessed the prognostic value of BROMO-10 in predicting the onset of CRPC. Fifty-five patients that developed metastasis after radical prostatectomy without any adjuvant or salvage therapy ("natural history cohort") treated at Johns Hopkins were evaluated using Kaplan-Meier analysis considering time to CRPC from metastatic onset. Upon metastatic onset, all patients received androgen deprivation therapy (ADT). Higher BROMO-10 scores were associated with an increased rate of CRPC after ADT (Figure 7C). The upper quartile of BROMO-10 signature scores had a median time to CRPC of 12 months compared to the lower quartile of 84 months ($p = 0.01$).

Finally, to assess whether BROMO-10 is able to predict responsiveness of PC to bromodomain inhibitors, we used RNA-seq profiles of panels of PC cell lines and expression array profiles of patient-derived xenografts (PDXs) (Nguyen et al., 2017) to generate BROMO-10 scores (Figures 7D and 7E). We then correlated these scores with publicly available IC_{50} data for JQ1 (Asangani et al., 2016) (Figure 7F), ZEN-3694 (Attwell

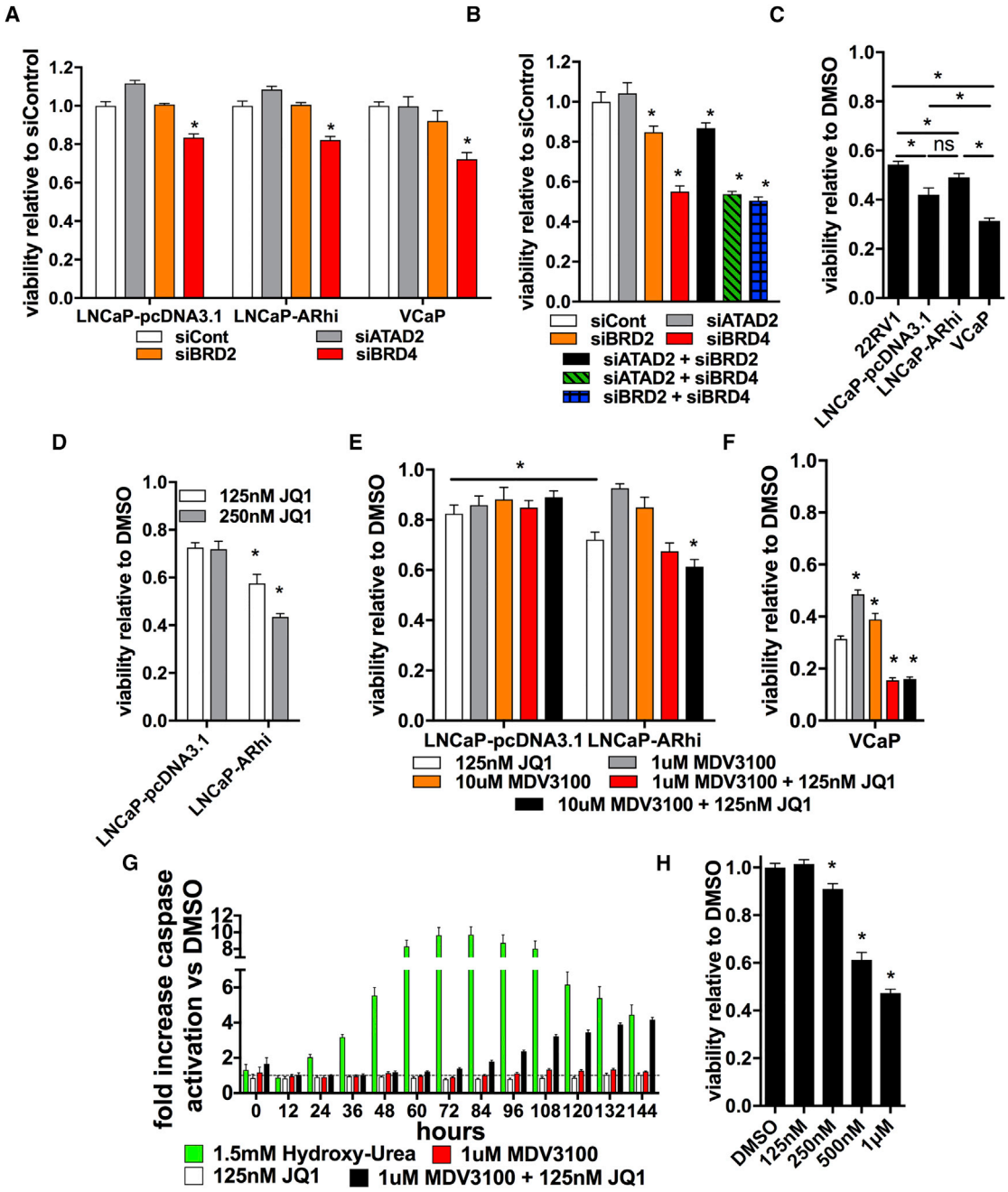

Figure 5. Impact of Bromodomain Inhibition on PC Cell Viability Is Enhanced by AR Deregulation

(A) Viability of LNCaP-pcDNA3.1, LNCaP-ARhi, and VCaP cells 3 days after transfection with siControl (siCont), siBRD2, siATAD2, or siBRD4, relative to control siRNA values.

(B) Viability of parental LNCaP cells 3 days after transfection with siRNA as indicated. *$p < 0.05$ according to t test versus the siCont column. n = 6 for each replicate, for each condition. Each experiment was repeated three times.

(C) Relative viability of 22RV1, LNCaP-pcDNA3.1, LNCaP-ARhi, and VCaP cells cultured in full serum and treated with DMSO or JQ1(*$p < 0.05$ according to t test between the indicated conditions).

(D) LNCaP-pcDNA3.1 and -ARhi cells were treated with 1 nM DHT as well as JQ1 or vehicle (DMSO).

(E and F) Solo or combinatorial treatment of LNCaP-pcDNA3.1 and LNCaP-ARhi cells (E) or VCaP cells (F) with MDV3100 and JQ1. Viability compared to DMSO was assessed after 3 days treatment (*$p < 0.05$ according to t test versus JQ1 treatment alone).

(G) Caspase activation assay upon treatment of VCaP cells with JQ1, MDV3100, or a combination; hydroxyl-urea was used as a positive control.

(H) Viability of MDV3100-resistant LNCaP cells treated with JQ1(*$p < 0.05$ according to t test versus DMSO).

Refer also to Figure S4.

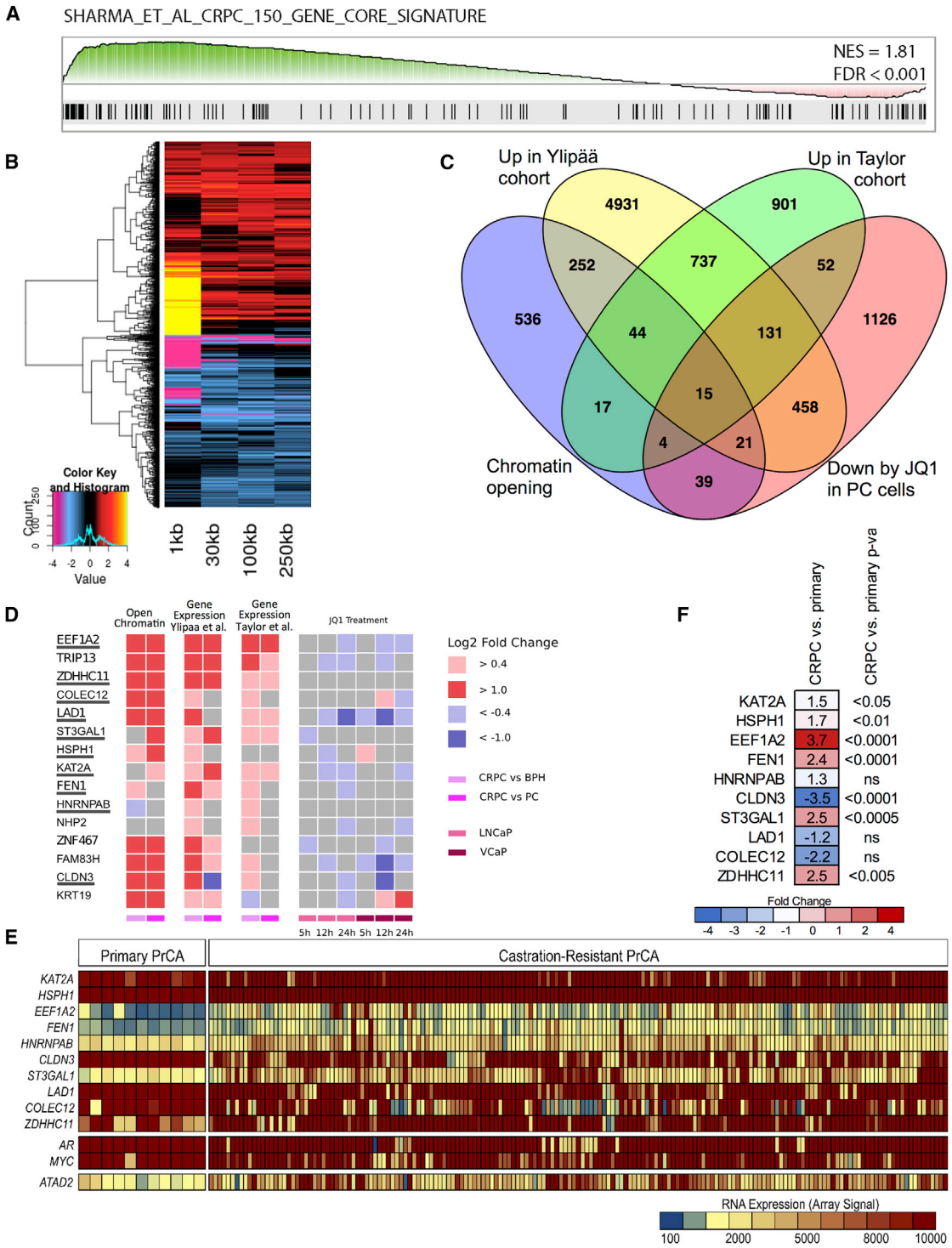

Figure 6. Bromodomain Inhibition Targets Clinically Relevant Transcriptional Program Useful for Selecting Patients Responsive to Bromodomain-Targeted Therapies

(A) GSEA of AR target gene signature (150 core genes identified in CRPC tissue) (Sharma et al., 2013) in expression analysis of VCaP cells treated with JQ1.

(B) Heatmap of genes displaying differential chromatin opening (varying distances upstream of TSSs) in CRPC versus primary PC.

(C) Overlaps between overexpressed genes in CRPC in two clinical microarray datasets (Tables S4A and S4B), the genes associated with open chromatin sites in CRPC (Table S5) and the consensus genes downregulated by JQ1 treatment of two cell lines (Table S2B).

(D) 15 genes associated with open chromatin, overexpressed in CRPC and downregulated by JQ1 treatment.

(legend continued on next page)

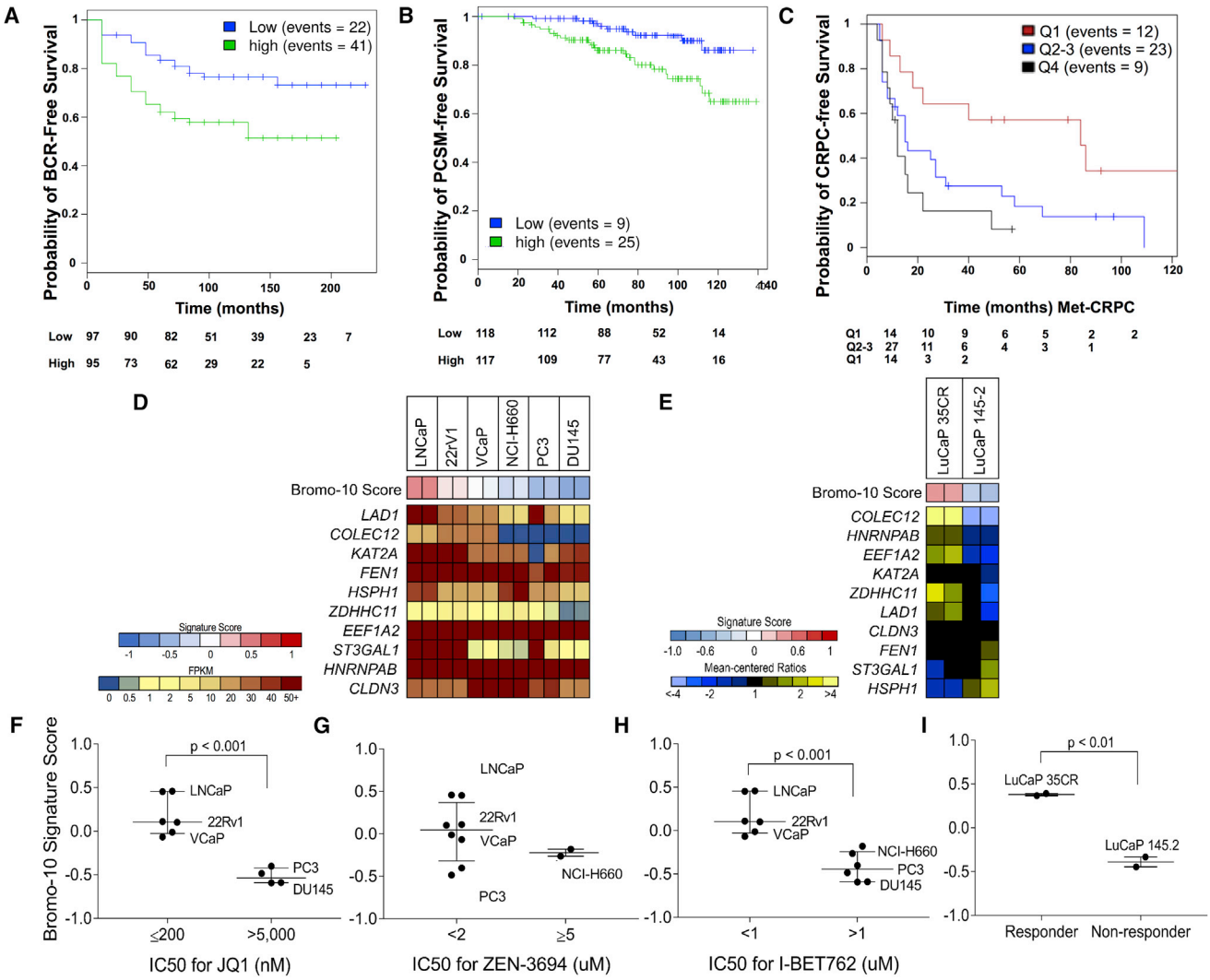

Figure 7. Prognostic and Predictive Value of the Ten Genes Signature BROMO-10

(A–C) Kaplan-Meier curves indicating the prognostic separation achieved by high and low BROMO-10 scores versus (A) biochemical recurrence in the JHMI-RP validation cohort (Ross et al., 2016) (p = 0.008) (B) prostate cancer-specific mortality (PCSM)-free survival in the Mayo Clinic validation cohort (Karnes et al., 2013) (p = 0.0089) and (C) CRPC-free survival of patients post-ADT treatment of metastatic patients in the JHMI cohort as expression quartiles (n = 55, p value 0.01).
(D and E) Heatmaps of BROMO-10 score and individual gene expression in cell lines (D) and also in PDX models (E).
(F–I) Two-sample t test evaluation of the significance of growth inhibition or reduction in tumor volume with IC_{50} dose administration of BET bromodomain inhibitors JQ1 (F), ZEN-3694 (G), and I-BET762 (H) to cell lines or of ZEN-3694 to PDX xenografts (I).
See Figure S6 and Table S6.

et al., 2016) (Figure 7G), I-BET762 (Figure 7H), and responsiveness to I-BET762 treatment measured as a significant reduction in tumor volume (Wyce et al., 2013) (Figure 7I). A high BROMO-10 score was significantly ($p < 0.001$) associated with responsiveness of PC cell lines to JQ1 and I-BET762 and reduction of tumor volume upon treatment of PC PDX models with I-BET762 ($p < 0.01$). However, the comparison between groups was not significant for responsiveness to ZEN-364 because PC3 cells, notably an AR negative PC cell line, had a low BROMO-10 score and was nevertheless sensitive to ZEN-364. Taken together, these data confirm the ability of BROMO-10 to predict responsiveness to BET inhibitors.

(E and F) Underlined genes were also significant as assessed in Fred Hutchinson Cancer Research Center (FHCRC) cohort comprising primary prostate cancers (PrCa; Roudier et al., 2016) and castration-resistant PrCa (Kumar et al., 2016) (E) with indicated fold-change values and p values according to a two-sample t test (F).
Refer also to Figure S5 and Tables S2, S3, S4, and S5.

DISCUSSION

Here, we show that chromatin accessibility increases during PC cancer progression due to mechanisms that involve the AR overexpression and the activity of BRDs. Importantly, we found that the chromatin structure in CRPC is able to classify disease stage demonstrating that genome-wide chromatin structure is reprogrammed as disease progresses, and it shows distinct features compared to primary tumors or benign tissue. Increased chromatin accessibility in PC was inferred in a recent study, although the low number of peaks found in the healthy tissue dominated the results (Stelloo et al., 2015). For the present study, we developed an advanced analysis pipeline to exclude possible confounding factors such as variations in ploidy from sample to sample (see Supplemental Information). This was essential for improved analyses because copy number variation has previously been shown to be strongly associated with poor prognosis in advance disease (Taylor et al., 2010).

Interestingly, androgens were able to enhance chromatin opening especially at ARBSs. This suggests a positive feedback loop in which the AR is able to bind more tightly to the genome due to increased opening at ARBSs. These data are concordant with our previous results showing stronger AR binding to chromatin in AR-overexpressing cells (Massie et al., 2011; Urbanucci et al., 2012b) and to other reports showing that chromatin accessibility is pre-docked prior AR binding at ARBSs (Andreu-Vieyra et al., 2011; He et al., 2010).

BRDs have gained extensive attention due to their tissue-specific capacity to modulate key transcriptional events during cancer progression (Fu et al., 2015) also in CRPC where they are therapeutically relevant (Asangani et al., 2014). We found that selected key BRDs such as ATAD2, BRD2, and BRD4 have a locus-specific effect on chromatin opening, suggesting that compensatory mechanisms may take place if BRDs are inhibited with single agents. For instance, we show that upregulation of the AR or MYC proteins occurs while inhibiting ATAD2 or BRD2 and possibly explains the limited effect of their inhibition on cell viability.

We also show that ATAD2 and BRD2 are androgen regulated. ATAD2 was previously reported to be androgen regulated (Zou et al., 2009). However, here we report that ATAD2 expression is enhanced in AR-overexpressing cells at low concentrations of androgens, and BRD4 long isoform, BRD2, and ATAD2 are all overexpressed in CRPC tissues. These results support the presence of an AR deregulation-mediated positive feedback loop that boosts the expression of BRDs in order to increase AR chromatin accessibility. Moreover, ATAD2 had strong prognostic value on a cohort of 10,000 patients. Our data also suggest that, while ATAD2 is an optimal tissue biomarker in identifying PC tissues where active transcription due to heavy cell-cycle turnover is ongoing, it may not be a good target for PC therapy, as also shown recently (Bamborough et al., 2016), if not targeted in combination with other agents such as antiandrogens.

The role of ATAD2 as a regulator of chromatin dynamics is well known in yeast (Cattaneo et al., 2014). A recent study showed that ATAD2 is highly expressed in replicating PC cells and ATAD2 expression correlates with expression of cell-cycle and DNA replication genes that have overlapping function in meiosis and tumor progression (Koo et al., 2016). Moreover, in highly proliferating embryonic stem cells, ATAD2 was reported to sustain specific gene expression programs via regulating chromatin opening guided by histone acetylation (Morozumi et al., 2016), which is in agreement with our data. These findings corroborate our data and are supportive of ATAD2 being a possible contributor to increased transcription plasticity in CRPC.

Our study also suggests that there might be a subpopulation of tumors that are more dependent on BRDs activity than others. Therefore, we built a ten-gene signature, BROMO-10, which is able to discriminate patients with poorer outcome, which takes into account chromatin structure and additionally incorporates key PC-specific downstream targets of BRDs. Interestingly, these targets include *FEN1*, which we have previously described to be important for PC progression and proposed as a tissue biomarker for biochemical recurrence (Urbanucci et al., 2012b), EEF1A2, which has been proposed as a marker of prostate cell transformation (Scaggiante et al., 2012; Sun et al., 2014), *KAT2A*, which encodes a histone acetyl-transferase controlling the PI3/AKT pathway with therapeutic potential in leukemia (Sun et al., 2015), and *HSPH1*, which enhances MYC transcription and drives B cell non-Hodgkin lymphoma (Zappasodi et al., 2015).

Mechanisms of resistance to BET inhibition have been reported. Therefore, it is extremely important to define patients that will respond to BET-inhibition therapies in combination with standard therapies to avoid resistance. We show that BROMO-10 is able to predict response to BET-inhibition therapies, but the use of this signature should be limited to tumors with intact AR signaling, and further studies are needed to refine the signature for different compounds.

In conclusion, we propose AR deregulation-driven chromatin structure as a key determinant of tumor progression. We describe the effect of BET inhibition on chromatin accessibility as an additional mechanism by which it is able to repress cell growth in a cell-specific manner. Moreover, we propose BROMO-10 signature to be used to select patients more likely to benefit from BET-targeted therapies and avoid recurrence. The selection of PC patients into future trials evaluating the efficacy should be based on the assessment of AR status, key BRDs expression, such as ATAD2, and the gene signature that reflects the chromatin status of these tumors.

EXPERIMENTAL PROCEDURES

Clinical Samples

All work on clinical samples has been carried out in compliance with the Helsinki Declaration and with the approval of ethics boards at collaborating institutions as outlined below. The tissue microarray from the Department of Urology and the Martini Clinics at the University Medical Centre Hamburg-Eppendorf consisted of archived diagnostic leftover tissues. Manufacture and analysis was approved by the local ethics committee (Ethics commission Hamburg, WF-049/09 and PV3652). According to local laws (HmbKHG, §12,1), informed consent was not required for this study. Patient records and information were anonymized and de-identified prior to analysis.

Three BPH, six primary PC, and three CRPCs were used for FAIRE-seq assays and FAIRE-qPCR assays. RNA-seq data from transcriptomes of 12 BPH, 28 untreated PCs, and 13 CRPCs, including the samples used for FAIRE-seq, were publicly available (Ylipää et al., 2015). These samples and the tissue

microarray described below were provided by Tampere University Hospital. The use of these samples for FAIRE-seq and of the tissue microarray was approved by the ethical committee of Tampere University Hospital and the National Authority for Medicolegal Affairs. Written informed consent was obtained from the subjects for sequencing the samples.

The Tampere patients' cohort of tissue microarrays (TMAs) contained 258 formalin-fixed paraffin-embedded prostatectomy and 121 CRPC specimens. A subset of the cohort was used to immunostain for ATAD2, BRD2, and BRD4. The Hamburg patients' TMA cohort contained 9,467 prostatectomy tissue specimens. Radical prostatectomy specimens were available from 12,427 patients. PSA values were measured following surgery, and PSA recurrence was defined as the time point when postoperative PSA was increasing from at least 0.2 ng/mL.

FAIREs

Two replicates were processed for each cell line and condition for subsequent sequencing analysis. Three to five replicates were processed for qPCR analysis. Four million cells were plated and hormone deprived for 4 days. Cells were then treated with R1881 or DHT for 4 hr. To perform tissue FAIRE from clinical material, 3 mL of PBS containing 2 × protease inhibitor (Roche) was added to 40 × 20-μm sections of freshly frozen tissue specimens. Downstream fixation and processing of both sample types are as described in the Supplemental Information.

FAIRE-Seq Analysis

Peak detection for FAIRE-seq was performed using model-based analysis of ChIP-seq (MACS) (Zhang et al., 2008) with default parameters using inputs of each of the FAIRE samples as controls and with F-Seq (Boyle et al., 2008). Refer to Supplemental Information for more detail.

Evaluation of the 15-Gene Signature Prognostic Value

Microarray data from the Decipher GRID were extracted for three radical prostatectomy cohorts from previously described (Erho et al., 2013; Karnes et al., 2013; Ross et al., 2016) validation studies. A classifier to distinguish between metastatic versus non-metastatic cancers was developed. The classifier was constructed from 15 genes (Figure 5C) using a generalized linear model with elastic net regularization as previously described (Erho et al., 2013). The model was generated using the MCI cohort (GSE46691) as training data. In the final model, ten of the 15 genes contributed to the model score with six positively associated and four negatively associated genes as determined by the regularized coefficients (see also Table S6). Scores were then generated for samples from the Mayo Clinic II (MCII) and JHMI-RP validation cohorts, and performance in each cohort was assessed using survival analysis.

BROMO-10 scores in cell lines and patients derived xenografts were calculated using GSVA Bioconductor package (https://www.bioconductor.org/packages/release/bioc/html/GSVA.html).

Statistics

Statistical analyses were performed using GraphPad Prism, MATLAB, and Microsoft Excel. All statistical tests were two-tailed with testing level thresholds of $\alpha = 0.05$.

ACCESSION NUMBERS

The accession number for the gene expression and FAIRE-seq data reported in this paper is GEO: GSE73989. The data analysis script referred to in the Supplementary Experimental Procedures has also been deposited and is accessible at https://github.com/dvbcfo/depth_track_window.

SUPPLEMENTAL INFORMATION

Supplemental Information includes six figures, six tables, and one data file and can be found with this article online at http://dx.doi.org/10.1016/j.celrep.2017.05.049.

AUTHOR CONTRIBUTIONS

A.U. wrote the manuscript. I.G.M. and A.U. designed the study and analyzed the data. A.U., T.T., S.M., C.B., K.K.K., X.S., and S.J.B. performed experiments and edited the manuscript. A.U., V.K., D.V., M.T., M.A., E.D., I.M.C., P.L., and N.E. performed the bioinformatic analyses and edited the manuscript. H.M.I., A.K., and F.S. assisted in the preparation of the revised manuscript. D.J.V.G., S. Knapp, S. Kregel, R.J.K., A.E.R., P.S.N., E.C., F.Y.F., E.M.S., K.E.K., and M.N. contributed reagents or data and edited the manuscript. G.S., T.S., and T.L.J.T. provided clinical material and edited the manuscript. I.M., T.V., and L.S. contributed reagents and edited the manuscript.

ACKNOWLEDGMENTS

We thank Ms. Päivi Martikainen for the skillful technical assistance. We acknowledge the last scientific contribution of our beloved Ms. Mariitta Vakkuri to this work. A.U. is supported by the South-East Norway Health Authorities (Helse Sor-Ost grant ID 2014040) at the Oslo University Hospital and the Norwegian Centre for Molecular Medicine. I.M. has been funded by the MLS (390000 and 143295), Helse Sor-Ost (2014040), Norwegian Research Council (230559), and the Faculty of Medicine at the Oslo University Hospital. P.S.N., E.C., and I.M.C. are supported by NIH grants P50CA097186 and P01CA163227, and the Prostate Cancer Foundation. H.M.I. is supported by the Norwegian Cancer Society (711072, 102032, and 4521627). S. Knapp is grateful for support by the SGC, a registered charity (number 1097737) that receives funds from AbbVie, Bayer Pharma AG, Boehringer Ingelheim, Canada Foundation for Innovation, Eshelman Institute for Innovation, Genome Canada, Innovative Medicines Initiative (EU/EFPIA), Janssen, Merck & Co., Novartis Pharma AG, Ontario Ministry of Economic Development and Innovation, Pfizer, São Paulo Research Foundation-FAPESP, Takeda, and the Wellcome Trust. The funders had no role in the study design, data collection and analysis, the decision to publish, or preparation of the article.

Received: September 11, 2016
Revised: April 1, 2017
Accepted: May 12, 2017
Published: June 6, 2017

REFERENCES

Andreu-Vieyra, C., Lai, J., Berman, B.P., Frenkel, B., Jia, L., Jones, P.A., and Coetzee, G.A. (2011). Dynamic nucleosome-depleted regions at androgen receptor enhancers in the absence of ligand in prostate cancer cells. Mol. Cell. Biol. *31*, 4648–4662.

Asangani, I.A., Dommeti, V.L., Wang, X., Malik, R., Cieslik, M., Yang, R., Escara-Wilke, J., Wilder-Romans, K., Dhanireddy, S., Engelke, C., et al. (2014). Therapeutic targeting of BET bromodomain proteins in castration-resistant prostate cancer. Nature *510*, 278–282.

Asangani, I.A., Wilder-Romans, K., Dommeti, V.L., Krishnamurthy, P.M., Apel, I.J., Escara-Wilke, J., Plymate, S.R., Navone, N.M., Wang, S., Feng, F.Y., and Chinnaiyan, A.M. (2016). BET bromodomain inhibitors enhance efficacy and disrupt resistance to AR antagonists in the treatment of prostate cancer. Mol. Cancer Res. *14*, 324–331.

Attwell, S., Jahagirdar, R., Norek, K., Calosing, C., Tsujikawa, L., Kharenko, O.A., Patel, R.G., Gesner, E.M., Corey, E., Nguyen, H.M., et al. (2016). Abstract LB-207: Preclinical characterization of ZEN-3694, a novel BET bromodomain inhibitor entering phase I studies for metastatic castration-resistant prostate cancer (mCRPC). Cancer Res. *76*, LB-207–LB-207.

Bamborough, P., Chung, C.W., Demont, E.H., Furze, R.C., Bannister, A.J., Che, K.H., Diallo, H., Douault, C., Grandi, P., Kouzarides, T., et al. (2016). A chemical probe for the ATAD2 bromodomain. Angew. Chem. Int. Ed. Engl. *55*, 11382–11386.

Boyle, A.P., Guinney, J., Crawford, G.E., and Furey, T.S. (2008). F-Seq: A feature density estimator for high-throughput sequence tags. Bioinformatics *24*, 2537–2538.

Buttigliero, C., Tucci, M., Bertaglia, V., Vignani, F., Bironzo, P., Di Maio, M., and Scagliotti, G.V. (2015). Understanding and overcoming the mechanisms of primary and acquired resistance to abiraterone and enzalutamide in castration resistant prostate cancer. Cancer Treat. Rev. *41*, 884–892.

Cattaneo, M., Morozumi, Y., Perazza, D., Boussouar, F., Jamshidikia, M., Rousseaux, S., Verdel, A., and Khochbin, S. (2014). Lessons from yeast on emerging roles of the ATAD2 protein family in gene regulation and genome organization. Mol. Cells *37*, 851–856.

Cedar, H., and Bergman, Y. (2012). Programming of DNA methylation patterns. Annu. Rev. Biochem. *81*, 97–117.

Center, M.M., Jemal, A., Lortet-Tieulent, J., Ward, E., Ferlay, J., Brawley, O., and Bray, F. (2012). International variation in prostate cancer incidence and mortality rates. Eur. Urol. *61*, 1079–1092.

Chen, Z., Lan, X., Thomas-Ahner, J.M., Wu, D., Liu, X., Ye, Z., Wang, L., Sunkel, B., Grenade, C., Chen, J., et al. (2015). Agonist and antagonist switch DNA motifs recognized by human androgen receptor in prostate cancer. EMBO J. *34*, 502–516.

Delmore, J.E., Issa, G.C., Lemieux, M.E., Rahl, P.B., Shi, J., Jacobs, H.M., Kastritis, E., Gilpatrick, T., Paranal, R.M., Qi, J., et al. (2011). BET bromodomain inhibition as a therapeutic strategy to target c-Myc. Cell *146*, 904–917.

Dolfini, D., and Mantovani, R. (2013). Targeting the Y/CCAAT box in cancer: YB-1 (YBX1) or NF-Y? Cell Death Differ. *20*, 676–685.

Erho, N., Crisan, A., Vergara, I.A., Mitra, A.P., Ghadessi, M., Buerki, C., Bergstralh, E.J., Kollmeyer, T., Fink, S., Haddad, Z., et al. (2013). Discovery and validation of a prostate cancer genomic classifier that predicts early metastasis following radical prostatectomy. PLoS ONE *8*, e66855.

Erzurumlu, Y., and Ballar, P. (2017). Androgen mediated regulation of endoplasmic reticulum-associated degradation and its effects on prostate cancer. Sci. Rep. *7*, 40719.

Filippakopoulos, P., and Knapp, S. (2014). Targeting bromodomains: Epigenetic readers of lysine acetylation. Nat. Rev. Drug Discov. *13*, 337–356.

Filippakopoulos, P., Picaud, S., Mangos, M., Keates, T., Lambert, J.P., Barsyte-Lovejoy, D., Felletar, I., Volkmer, R., Müller, S., Pawson, T., et al. (2012). Histone recognition and large-scale structural analysis of the human bromodomain family. Cell *149*, 214–231.

Fu, L.L., Tian, M., Li, X., Li, J.J., Huang, J., Ouyang, L., Zhang, Y., and Liu, B. (2015). Inhibition of BET bromodomains as a therapeutic strategy for cancer drug discovery. Oncotarget *6*, 5501–5516.

Giresi, P.G., and Lieb, J.D. (2009). Isolation of active regulatory elements from eukaryotic chromatin using FAIRE (formaldehyde assisted isolation of regulatory elements). Methods *48*, 233–239.

He, H.H., Meyer, C.A., Shin, H., Bailey, S.T., Wei, G., Wang, Q., Zhang, Y., Xu, K., Ni, M., Lupien, M., et al. (2010). Nucleosome dynamics define transcriptional enhancers. Nat. Genet. *42*, 343–347.

Karnes, R.J., Bergstralh, E.J., Davicioni, E., Ghadessi, M., Buerki, C., Mitra, A.P., Crisan, A., Erho, N., Vergara, I.A., Lam, L.L., et al. (2013). Validation of a genomic classifier that predicts metastasis following radical prostatectomy in an at risk patient population. J. Urol. *190*, 2047–2053.

Koo, S.J., Fernández-Montalván, A.E., Badock, V., Ott, C.J., Holton, S.J., von Ahsen, O., Toedling, J., Vittori, S., Bradner, J.E., and Gorjánácz, M. (2016). ATAD2 is an epigenetic reader of newly synthesized histone marks during DNA replication. Oncotarget *7*, 70323–70335.

Kregel, S., Kiriluk, K.J., Rosen, A.M., Cai, Y., Reyes, E.E., Otto, K.B., Tom, W., Paner, G.P., Szmulewitz, R.Z., and Vander Griend, D.J. (2013). Sox2 is an androgen receptor-repressed gene that promotes castration-resistant prostate cancer. PLoS ONE *8*, e53701.

Kumar, A., Coleman, I., Morrissey, C., Zhang, X., True, L.D., Gulati, R., Etzioni, R., Bolouri, H., Montgomery, B., White, T., et al. (2016). Substantial interindividual and limited intraindividual genomic diversity among tumors from men with metastatic prostate cancer. Nat. Med. *22*, 369–378.

Lever, E., and Sheer, D. (2010). The role of nuclear organization in cancer. J. Pathol. *220*, 114–125.

Lovén, J., Hoke, H.A., Lin, C.Y., Lau, A., Orlando, D.A., Vakoc, C.R., Bradner, J.E., Lee, T.I., and Young, R.A. (2013). Selective inhibition of tumor oncogenes by disruption of super-enhancers. Cell *153*, 320–334.

Massie, C.E., Lynch, A., Ramos-Montoya, A., Boren, J., Stark, R., Fazli, L., Warren, A., Scott, H., Madhu, B., Sharma, N., et al. (2011). The androgen receptor fuels prostate cancer by regulating central metabolism and biosynthesis. EMBO J. *30*, 2719–2733.

Morozumi, Y., Boussouar, F., Tan, M., Chaikuad, A., Jamshidikia, M., Colak, G., He, H., Nie, L., Petosa, C., de Dieuleveult, M., et al. (2016). Atad2 is a generalist facilitator of chromatin dynamics in embryonic stem cells. J. Mol. Cell Biol. *8*, 349–362.

Nagarajan, S., Hossan, T., Alawi, M., Najafova, Z., Indenbirken, D., Bedi, U., Taipaleenmäki, H., Ben-Batalla, I., Scheller, M., Loges, S., et al. (2014). Bromodomain protein BRD4 is required for estrogen receptor-dependent enhancer activation and gene transcription. Cell Rep. *8*, 460–469.

Nguyen, H.M., Vessella, R.L., Morrissey, C., Brown, L.G., Coleman, I.M., Higano, C.S., Mostaghel, E.A., Zhang, X., True, L.D., Lam, H.M., et al. (2017). LuCaP prostate cancer patient-derived xenografts reflect the molecular heterogeneity of advanced disease and serve as models for evaluating cancer therapeutics. Prostate *77*, 654–671.

Perry, A.S., Watson, R.W., Lawler, M., and Hollywood, D. (2010). The epigenome as a therapeutic target in prostate cancer. Nat. Rev. Urol. *7*, 668–680.

Pomerantz, M.M., Li, F., Takeda, D.Y., Lenci, R., Chonkar, A., Chabot, M., Cejas, P., Vazquez, F., Cook, J., Shivdasani, R.A., et al. (2015). The androgen receptor cistrome is extensively reprogrammed in human prostate tumorigenesis. Nat. Genet. *47*, 1346–1351.

Ross, A.E., Johnson, M.H., Yousefi, K., Davicioni, E., Netto, G.J., Marchionni, L., Fedor, H.L., Glavaris, S., Choeurng, V., Buerki, C., et al. (2016). Tissue-based genomics augments post-prostatectomy risk stratification in a natural history cohort of intermediate- and high-risk men. Eur. Urol.

Roudier, M.P., Winters, B.R., Coleman, I., Lam, H.M., Zhang, X., Coleman, R., Chéry, L., True, L.D., Higano, C.S., Montgomery, B., et al. (2016). Characterizing the molecular features of ERG-positive tumors in primary and castration resistant prostate cancer. Prostate *76*, 810–822.

Scaggiante, B., Dapas, B., Bonin, S., Grassi, M., Zennaro, C., Farra, R., Cristiano, L., Siracusano, S., Zanconati, F., Giansante, C., and Grassi, G. (2012). Dissecting the expression of EEF1A1/2 genes in human prostate cancer cells: The potential of EEF1A2 as a hallmark for prostate transformation and progression. Br. J. Cancer *106*, 166–173.

Sharma, N.L., Massie, C.E., Ramos-Montoya, A., Zecchini, V., Scott, H.E., Lamb, A.D., MacArthur, S., Stark, R., Warren, A.Y., Mills, I.G., and Neal, D.E. (2013). The androgen receptor induces a distinct transcriptional program in castration-resistant prostate cancer in man. Cancer Cell *23*, 35–47.

Shi, J., and Vakoc, C.R. (2014). The mechanisms behind the therapeutic activity of BET bromodomain inhibition. Mol. Cell *54*, 728–736.

Song, L., Zhang, Z., Grasfeder, L.L., Boyle, A.P., Giresi, P.G., Lee, B.K., Sheffield, N.C., Gräf, S., Huss, M., Keefe, D., et al. (2011). Open chromatin defined by DNaseI and FAIRE identifies regulatory elements that shape cell-type identity. Genome Res. *21*, 1757–1767.

Stelloo, S., Nevedomskaya, E., van der Poel, H.G., de Jong, J., van Leenders, G.J., Jenster, G., Wessels, L.F., Bergman, A.M., and Zwart, W. (2015). Androgen receptor profiling predicts prostate cancer outcome. EMBO Mol. Med. *7*, 1450–1464.

Sun, Y., Du, C., Wang, B., Zhang, Y., Liu, X., and Ren, G. (2014). Up-regulation of eEF1A2 promotes proliferation and inhibits apoptosis in prostate cancer. Biochem. Biophys. Res. Commun. *450*, 1–6.

Sun, X.J., Man, N., Tan, Y., Nimer, S.D., and Wang, L. (2015). The role of histone acetyltransferases in normal and malignant hematopoiesis. Front. Oncol. *5*, 108.

Tark-Dame, M., Jerabek, H., Manders, E.M., van der Wateren, I.M., Heermann, D.W., and van Driel, R. (2014). Depletion of the chromatin looping proteins CTCF and cohesin causes chromatin compaction: Insight into chromatin folding by polymer modelling. PLoS Comput. Biol. *10*, e1003877.

Taylor, B.S., Schultz, N., Hieronymus, H., Gopalan, A., Xiao, Y., Carver, B.S., Arora, V.K., Kaushik, P., Cerami, E., Reva, B., et al. (2010). Integrative genomic profiling of human prostate cancer. Cancer Cell *18*, 11–22.

Tewari, A.K., Yardimci, G.G., Shibata, Y., Sheffield, N.C., Song, L., Taylor, B.S., Georgiev, S.G., Coetzee, G.A., Ohler, U., Furey, T.S., et al. (2012). Chromatin accessibility reveals insights into androgen receptor activation and transcriptional specificity. Genome Biol. *13*, R88.

Timp, W., and Feinberg, A.P. (2013). Cancer as a dysregulated epigenome allowing cellular growth advantage at the expense of the host. Nat. Rev. Cancer *13*, 497–510.

Urbanucci, A., Marttila, S., Janne, O.A., and Visakorpi, T. (2012a). Androgen receptor overexpression alters binding dynamics of the receptor to chromatin and chromatin structure. Prostate.

Urbanucci, A., Sahu, B., Seppälä, J., Larjo, A., Latonen, L.M., Waltering, K.K., Tammela, T.L., Vessella, R.L., Lähdesmäki, H., Jänne, O.A., and Visakorpi, T. (2012b). Overexpression of androgen receptor enhances the binding of the receptor to the chromatin in prostate cancer. Oncogene *31*, 2153–2163.

Urbanucci, A., Waltering, K., Mills, I., and Visakorpi, T. (2013). The effect of AR overexpression on androgen signaling in prostate cancer. In Androgen-Responsive Genes in Prostate Cancer, Z. Wang, ed. (Springer), pp. 187–200.

Waltering, K.K., Helenius, M.A., Sahu, B., Manni, V., Linja, M.J., Jänne, O.A., and Visakorpi, T. (2009). Increased expression of androgen receptor sensitizes prostate cancer cells to low levels of androgens. Cancer Res. *69*, 8141–8149.

Waltering, K.K., Urbanucci, A., and Visakorpi, T. (2012). Androgen receptor (AR) aberrations in castration-resistant prostate cancer. Mol. Cell. Endocrinol. *360*, 38–43.

Wyce, A., Degenhardt, Y., Bai, Y., Le, B., Korenchuk, S., Crouthamel, M.-C., McHugh, C., Vessella, R., Creasy, C., Tummino, P., et al. (2013). Inhibition of BET bromodomain proteins as a therapeutic approach in prostate cancer. Oncotarget *4*, 2419–2429.

Xu, Y., Dalrymple, S.L., Becker, R.E., Denmeade, S.R., and Isaacs, J.T. (2006). Pharmacologic basis for the enhanced efficacy of dutasteride against prostatic cancers. Clin. Cancer Res. *12*, 4072–4079.

Ylipää, A., Kivinummi, K., Kohvakka, A., Annala, M., Latonen, L., Scaravilli, M., Kartasalo, K., Leppänen, S.P., Karakurt, S., Seppälä, J., et al. (2015). Transcriptome sequencing reveals PCAT5 as a novel ERG-regulated long noncoding RNA in prostate cancer. Cancer Res. *75*, 4026–4031.

Yu, J., Yu, J., Mani, R.S., Cao, Q., Brenner, C.J., Cao, X., Wang, X., Wu, L., Li, J., Hu, M., et al. (2010). An integrated network of androgen receptor, polycomb, and TMPRSS2-ERG gene fusions in prostate cancer progression. Cancer Cell *17*, 443–454.

Zappasodi, R., Ruggiero, G., Guarnotta, C., Tortoreto, M., Tringali, C., Cavanè, A., Cabras, A.D., Castagnoli, L., Venerando, B., Zaffaroni, N., et al. (2015). HSPH1 inhibition downregulates Bcl-6 and c-Myc and hampers the growth of human aggressive B-cell non-Hodgkin lymphoma. Blood *125*, 1768–1771.

Zhang, Y., Liu, T., Meyer, C.A., Eeckhoute, J., Johnson, D.S., Bernstein, B.E., Nusbaum, C., Myers, R.M., Brown, M., Li, W., and Liu, X.S. (2008). Model-based analysis of ChIP-Seq (MACS). Genome Biol. *9*, R137.

Zhang, T.Y., Agarwal, N., Sonpavde, G., DiLorenzo, G., Bellmunt, J., and Vogelzang, N.J. (2013). Management of castrate resistant prostate cancer-recent advances and optimal sequence of treatments. Curr. Urol. Rep. *14*, 174–183.

Zou, J.X., Guo, L., Revenko, A.S., Tepper, C.G., Gemo, A.T., Kung, H.J., and Chen, H.W. (2009). Androgen-induced coactivator ANCCA mediates specific androgen receptor signaling in prostate cancer. Cancer Res. *69*, 3339–3346.